

**Supporting information for:
Potential of Polarizable Force Fields for
Predicting the Separation Performance of
Small Hydrocarbons in M-MOF-74**

Tim M. Becker,[†] Azahara Luna-Triguero,[‡] Jose Manuel Vicent-Luna,[‡] Li-Chiang Lin,[¶] David Dubbeldam,^{†,§} Sofia Calero,[‡] and Thijs J. H. Vlugt^{*,†}

Engineering Thermodynamics, Process & Energy Department, Faculty of Mechanical, Maritime and Materials Engineering, Delft University of Technology, Leeghwaterstraat 39, 2628CB Delft, The Netherlands, Department of Physical, Chemical and Natural Systems, Universidad Pablo de Olavide, Ctra. Utrera km 1. ES-41013, Seville, Spain, William G. Lowrie Department of Chemical and Biomolecular Engineering, The Ohio State University, 151 W. Woodruff Ave., Columbus, OH 43210, United States, and Van't Hoff Institute for Molecular Sciences, University of Amsterdam, Science Park 904, 1098XH Amsterdam, The Netherlands

E-mail: t.j.h.vlugt@tudelft.nl

^{*}To whom correspondence should be addressed

[†]Delft University of Technology

[‡]Universidad Pablo de Olavide

[¶]The Ohio State University

[§]University of Amsterdam

Supporting Information Available

The Electronic Supplementary Information consists of 6 parts. The first part summarizes all force field parameters adopted in this study. Tables S1 to S4 provide the parameters for the M-MOF-74 frameworks. Tables S5 to S12 summarize the force field parameters of the adsorbates. In Figure S1, a representation of all considered interaction sites of M-MOF-74 with labels is provided. In the second part, a schematic view of the binding geometry for C3 hydrocarbons is shown (Figure S2). Subsequently, the binding geometries for all systems are provided (Figures S3 to S6). Next, adsorption isotherms calculated using the force field of Liu et al.^{S1} with the addition of explicit polarization are shown. In part 5, the details of the force field (Table S13) and the results of the calculations of Co-MOF-74 using charges determined via the charge equilibration (QEeq) method are provided (Figures S11 to S14). Finally, the energy surfaces determined for the plane of maximum energy are shown in Figures S15 to S18.

Force field parameters

Table S1: Force field parameters for Co-MOF-74. The charges are taken from previous studies^{S2–S4}. The framework is considered to be rigid.

#	Atom type	ε / k_B [K]	σ [\AA]	Partial charge [e]
1	Co	7.045	2.56	1.189
2	O1	47.86	3.473	-0.720
3	O2	47.86	3.473	-0.673
4	O3	47.86	3.473	-0.725
5	C1	48.19	3.033	0.846
6	C2	48.19	3.033	-0.308
7	C3	48.19	3.033	0.391
8	C4	48.19	3.033	-0.177
9	H	7.65	2.846	0.177

Table S2: Force field parameters for Fe-MOF-74. The charges are taken from previous studies^{S2–S4}. The framework is considered to be rigid.

#	Atom type	ε /k_B [K]	σ [\AA]	Partial charge [e]
1	Fe	6.54	2.59	1.288
2	O1	47.86	3.473	-0.753
3	O2	47.86	3.473	-0.707
4	O3	47.86	3.473	-0.794
5	C1	48.19	3.033	0.870
6	C2	48.19	3.033	-0.337
7	C3	48.19	3.033	0.432
8	C4	48.19	3.033	-0.195
9	H	7.65	2.846	0.196

Table S3: Force field parameters for Mn-MOF-74. The charges are taken from previous studies^{S2–S4}. The framework is considered to be rigid.

#	Atom type	ε /k_B [K]	σ [\AA]	Partial charge [e]
1	Mn	6.54	2.64	1.343
2	O1	47.86	3.473	-0.754
3	O2	47.86	3.473	-0.717
4	O3	47.86	3.473	-0.806
5	C1	48.19	3.033	0.850
6	C2	48.19	3.033	-0.296
7	C3	48.19	3.033	0.396
8	C4	48.19	3.033	-0.203
9	H	7.65	2.846	0.187

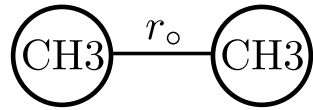
Table S4: Force field parameters for Ni-MOF-74. The charges are taken from previous studies^{S2–S4}. The framework is considered to be rigid.

#	Atom type	ε /k_B [K]	σ [\AA]	Partial charge [e]
1	Ni	7.55	2.52	1.298
2	O1	47.86	3.473	-0.789
3	O2	47.86	3.473	-0.696
4	O3	47.86	3.473	-0.785
5	C1	48.19	3.033	0.895
6	C2	48.19	3.033	-0.349
7	C3	48.19	3.033	0.418
8	C4	48.19	3.033	-0.173
9	H	7.65	2.846	0.181

Table S5: Force field parameters and atomic polarizabilities for ethane. Atomic polarizabilities are taken from Stout and Dykstra^{S5}.

#	Atom type	ε / k_B [K]	σ [\AA]	α [\AA ³]	Partial charge [e]
TraPPE ^{S6}	CH3	98.0	3.75	-	-
Liu ^{S1}	CH3	108.0	3.76	-	-
Pol. force field	CH3	98.0	3.75	1.874	-

Table S6: Geometries used for ethane. Bending potential according to $U^{\text{bend}} = \frac{1}{2} \cdot k_{\circ} \cdot (r - r_{\circ})^2$

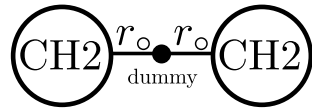


#	r_{\circ} / [Å]	k_{\circ}/k_B [K/Å ²]
TraPPE	1.54	rigid
Liu	1.54	96500
Pol. force field	1.54	rigid

Table S7: Force field parameters and atomic polarizabilities for ethylene. Atomic polarizabilities are taken from Stout and Dykstra^{S5}.

#	Atom type	ε / k_B [K]	σ [\AA]	α [\AA^3]	Partial charge [e]
TraPPE ^{S6}	CH2	85.0	3.675	-	-
Liu ^{S1}	CH2	93.0	3.685	-	-
Pol. force field	CH2	93.0	3.722	1.959	0.73
Pol. force field	dummy	0.0	0.0	-	-1.46
No charges	CH2	85.0	3.675	1.959	-
No polarization ^{S7}	CH2	93.0	3.722	-	0.73
No polarization ^{S7}	dummy	0.0	0.0	-	-1.46

Table S8: Geometries used for ethylene. Bending potential according to $U^{\text{bend}} = \frac{1}{2} \cdot k_{\circ} \cdot (r - r_{\circ})^2$

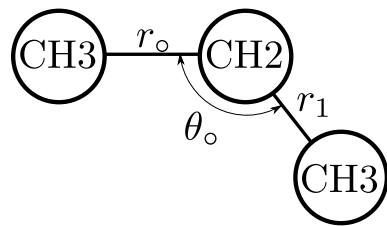


#	r_{\circ} / [\AA]	k_{\circ}/k_B / [K/ \AA^2]
TraPPE	0.6665	rigid
Liu	0.6665	96500
Pol. force field	0.6695	rigid
No charges	0.6665	rigid
No polarization	0.6695	rigid

Table S9: Force field parameters and atomic polarizabilities for propane. Atomic polarizabilities are taken from Stout and Dykstra^{S5}.

#	Atom type	$\varepsilon / k_B / [\text{K}]$	$\sigma [\text{\AA}]$	$\alpha [\text{\AA}^3]$	Partial charge [e]
TraPPE ^{S6}	CH3	98.0	3.75	-	-
TraPPE ^{S6}	CH2	46.0	3.95	-	-
Liu ^{S1}	CH3	108.0	3.76	-	-
Liu ^{S1}	CH2	56.0	3.96	-	-
Pol. force field	CH3	98.0	3.75	1.874	-
Pol. force field	CH2	46.0	3.95	1.874	-

Table S10: Geometries used for propane. Bond potential according to $U^{\text{bond}} = \frac{1}{2} \cdot k_{\circ} \cdot (r - r_{\circ})^2$ and bending according to $U^{\text{bend}} = \frac{1}{2} \cdot k_{\theta} \cdot (\theta - \theta_{\circ})^2$.

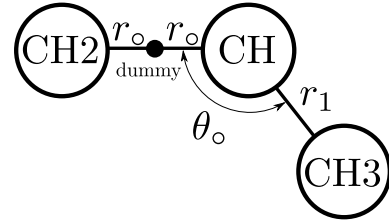


#	r_{\circ} / [Å]	k_{\circ}/k_B [K/Å ²]	r_1 / [Å]	p_1/k_B [K/Å ²]	θ_{\circ} / [°]	k_{θ}/k_B [K/rad ²]
TraPPE	1.54	rigid	1.54	rigid	114	62500
Liu	1.54	96500	1.54	96500	114	62500
Pol. force field	1.54	rigid	1.54	rigid	114	62500

Table S11: Force field parameters and atomic polarizabilities for propylene. Atomic polarizabilities are taken from Stout and Dykstra^{S5}.

#	Atom type	ε / k_B [K]	σ [\AA]	α [\AA ³]	Partial charge [e]
TraPPE ^{S6}	CH3	98.0	3.75	-	-
TraPPE ^{S6}	CH	47.0	3.73	-	-
TraPPE ^{S6}	CH2	85.0	3.675	-	-
Liu ^{S1}	CH3	108.0	3.76	-	-
Liu ^{S1}	CH	53.0	3.74	-	-
Liu ^{S1}	CH2	93.0	3.685	-	-
Pol. force field	CH3	108.0	3.76	1.874	-
Pol. force field	CH	53.0	3.74	1.959	0.87
Pol. force field	CH2	93.0	3.685	1.959	0.87
Pol. force field	dummy	0.0	0.0	-	-1.74
No charges	CH3	98.0	3.75	1.874	-
No charges	CH	47.0	3.73	1.959	-
No charges	CH2	85.0	3.675	1.959	-
No polarization ^{S8}	CH3	108.0	3.76	-	-
No polarization ^{S8}	CH	53.0	3.74	-	0.87
No polarization ^{S8}	CH2	93.0	3.685	-	0.87
No polarization ^{S8}	dummy	0.0	0.0	-	-1.74

Table S12: Geometries used for propylene. Bond potential according to $U^{\text{bond}} = \frac{1}{2} \cdot k_{\circ} \cdot (r - r_{\circ})^2$ and bending according to $U^{\text{bend}} = \frac{1}{2} \cdot k_{\theta} \cdot (\theta - \theta_{\circ})^2$.



#	r_{\circ} / [Å]	k_{\circ}/k_B [K/Å ²]	r_1 / [Å]	p_1/k_B [K/Å ²]	θ_{\circ} / [°]	k_{θ}/k_B [K/rad ²]
TraPPE	0.665	rigid	1.54	rigid	119.7	70420
Liu	0.665	96500	1.54	96500	119.7	70420
Pol. force field	0.704	rigid	1.54	96500	119.7	70420
No charges	0.665	rigid	1.54	rigid	119.7	70420
No polarization	0.704	rigid	1.54	96500	119.7	70420

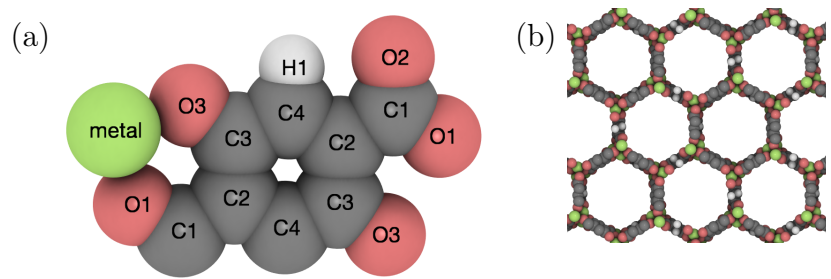


Figure S1: (a) Labeling of the interaction sites and (b) the framework of Mg-MOF-74. Magnesium, carbon, oxygen, and hydrogen are depicted in green, gray, red, and white, respectively.

Representation of binding geometry for C₃ hydrocarbons

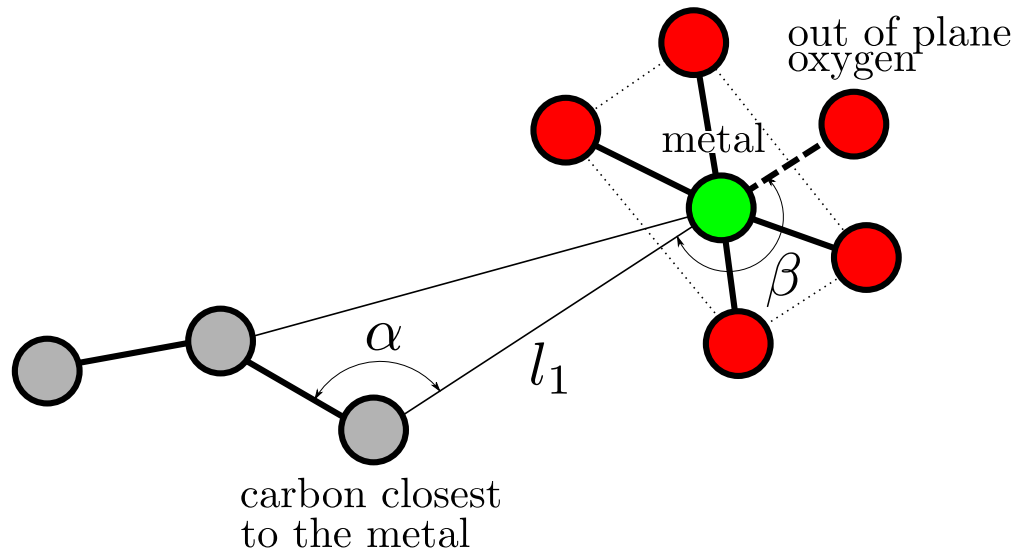


Figure S2: Schematic representation of the binding geometry for C₃ hydrocarbons within M-MOF-74. Carbon atoms, the metal atom, and oxygen atoms are colored in grey, green, and red, respectively.

Binding Geometries

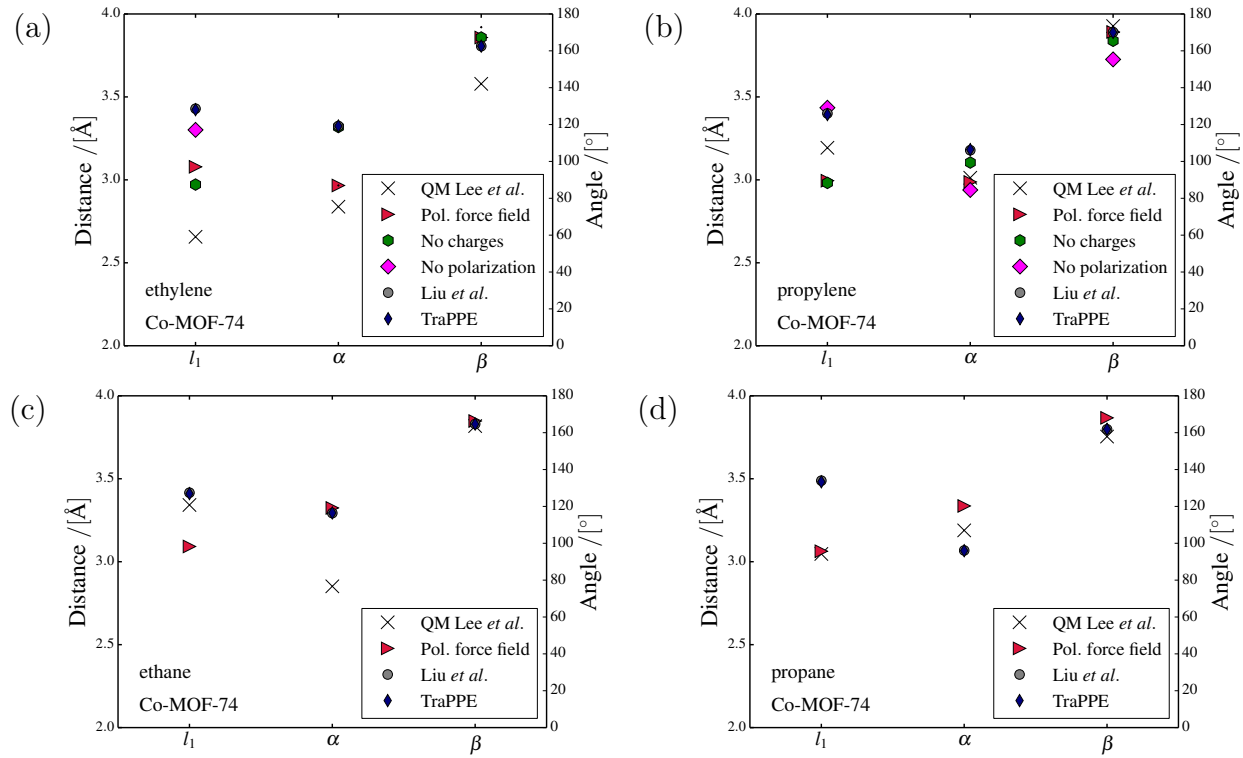


Figure S3: Summary of parameters to describe the binding geometry in Co-MOF-74. Comparison between several classical force fields and the DFT results of Lee et al.^{S3}. Parameters are defined according to Figure 2 of the main text.

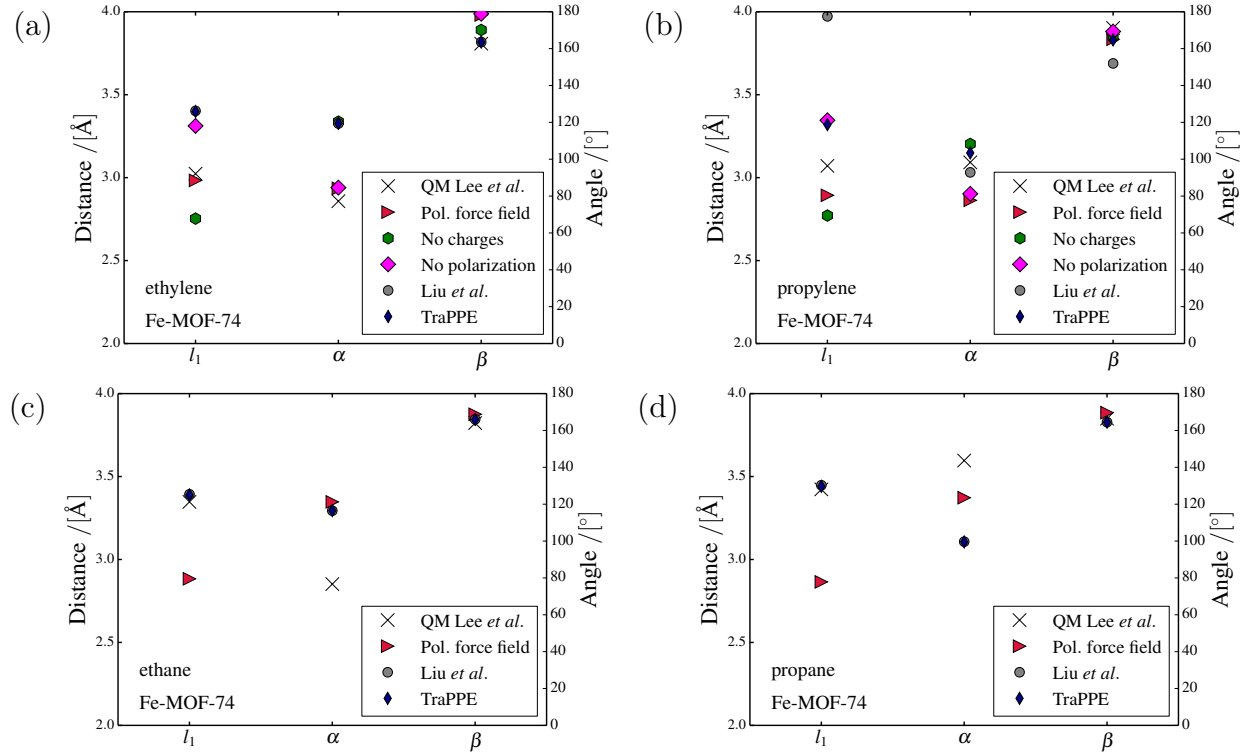


Figure S4: Summary of parameters to describe the binding geometry in Fe-MOF-74. Comparison between several classical force fields and the DFT results of Lee et al.^{S3}. Parameters are defined according to Figure 2 of the main text.

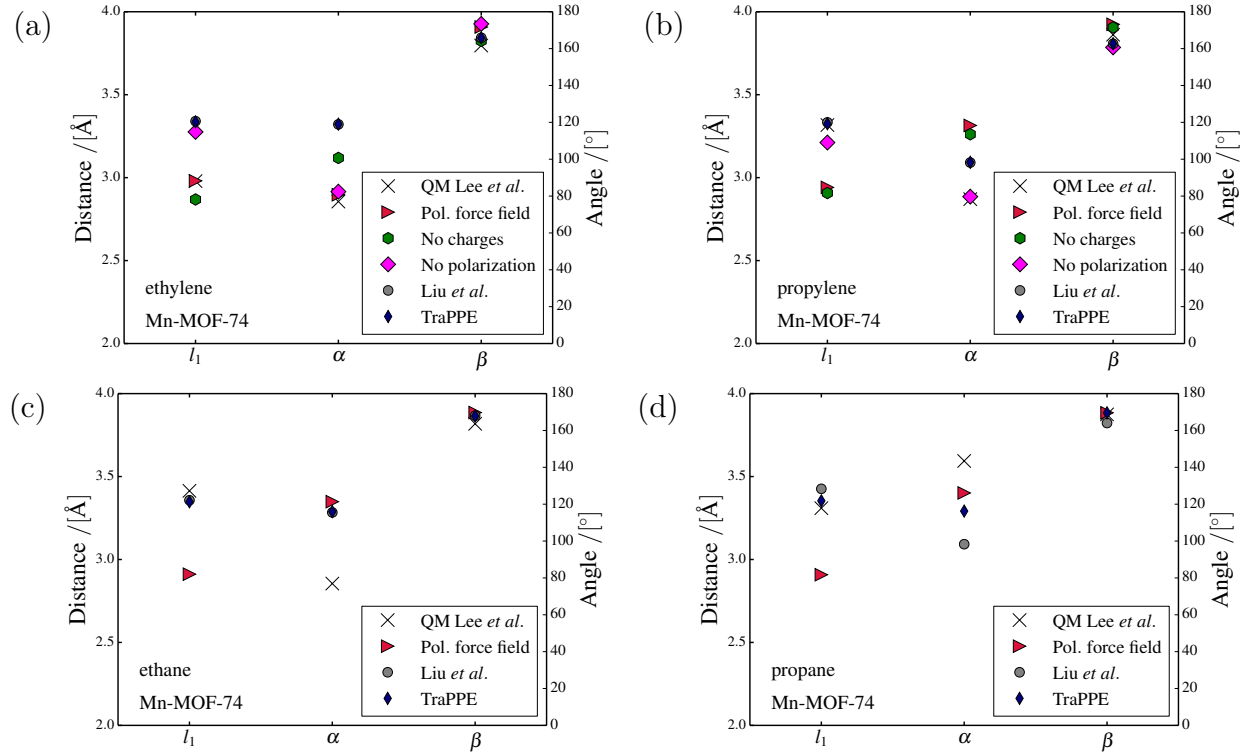


Figure S5: Summary of parameters to describe the binding geometry in Mn-MOF-74. Comparison between several classical force fields and the DFT results of Lee et al.^{S3}. Parameters are defined according to Figure 2 of the main text.

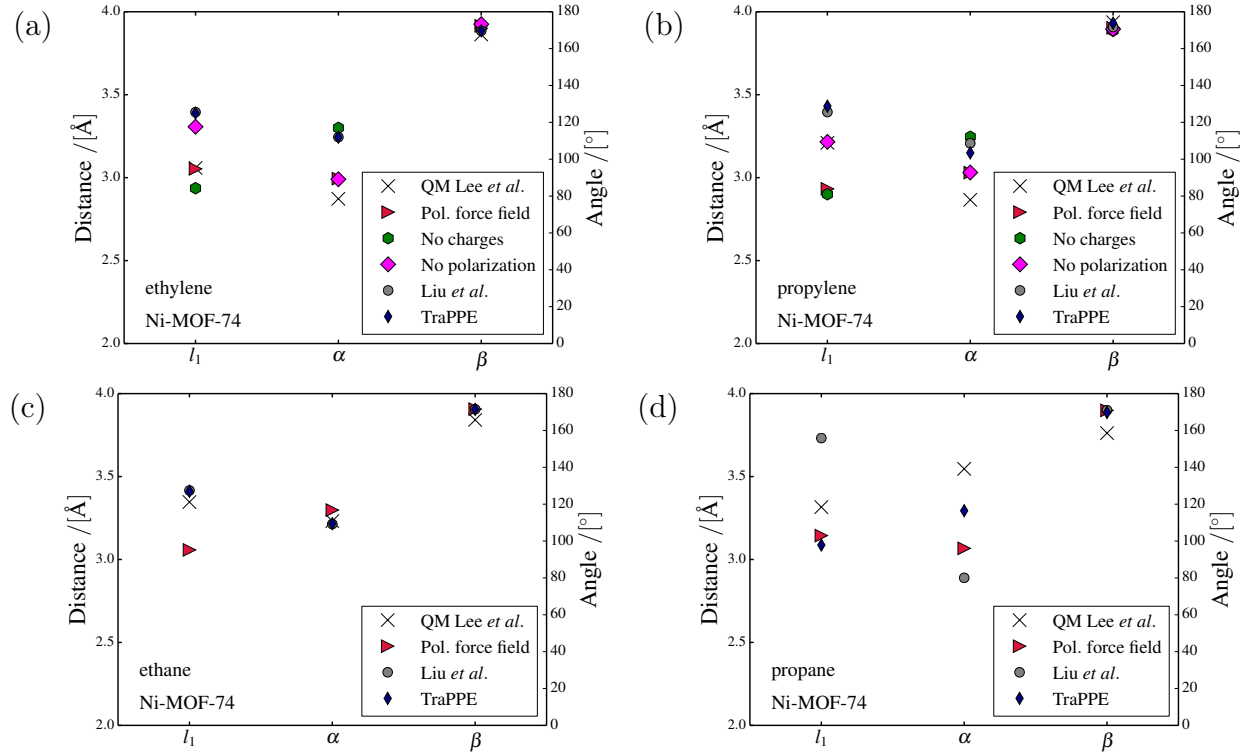


Figure S6: Summary of parameters to describe the binding geometry in Ni-MOF-74. Comparison between several classical force fields and the DFT results of Lee *et al.*^{S3}. Parameters are defined according to Figure 2 of the main text.

Adsorption isotherms with the force field of Liu et al.^{S1}
and additional polarization

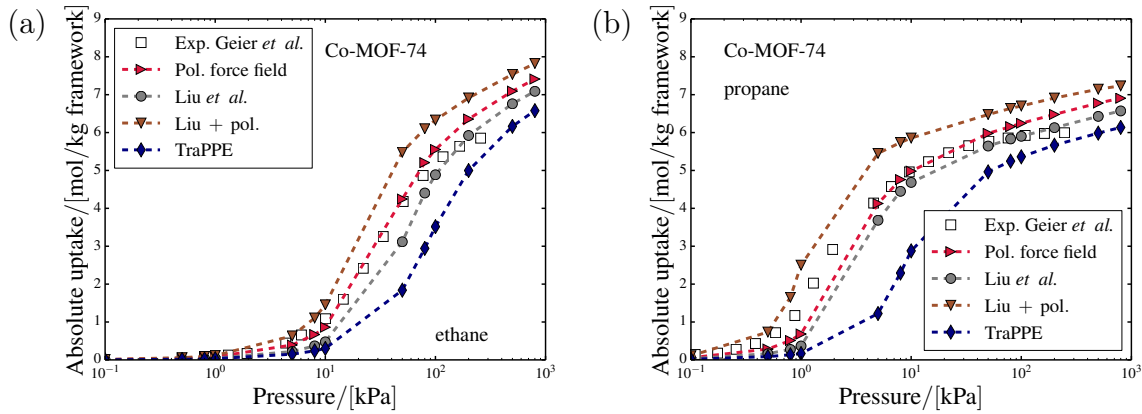


Figure S7: Adsorption isotherm for (a) ethane and (b) propane in Co-MOF-74 at 318 K predicted with the force field of Liu et al.^{S1} with and without adding explicit polarization. Comparison with the polarizable force field, the TraPPE force field^{S6}, and the experimental values of Geier et al.^{S9}.

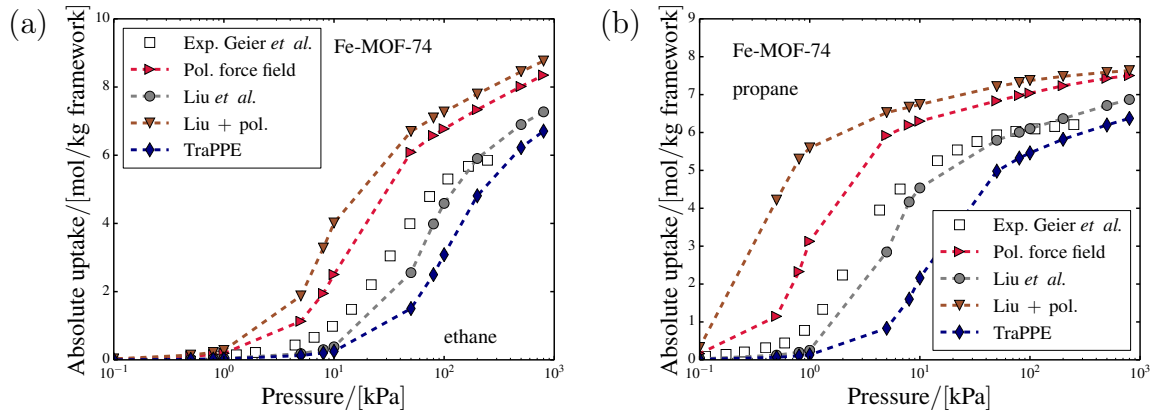


Figure S8: Adsorption isotherm for (a) ethane and (b) propane in Fe-MOF-74 at 318 K predicted with the force field of Liu *et al.*^{S1} with and without adding explicit polarization. Comparison with the polarizable force field, the TraPPE force field^{S6}, and the experimental values of Geier *et al.*^{S9}.

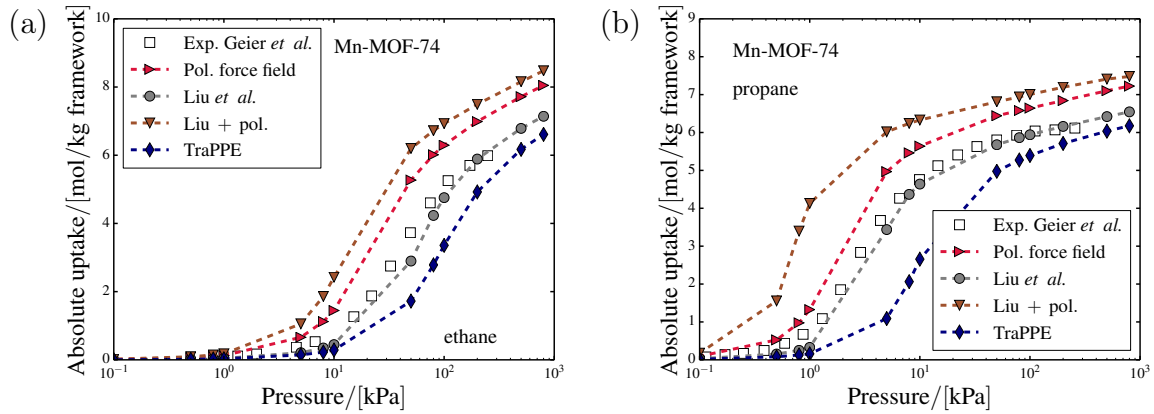


Figure S9: Adsorption isotherm for (a) ethane and (b) propane in Mn-MOF-74 at 318 K predicted with the force field of Liu et al.^{S1} with and without adding explicit polarization. Comparison with the polarizable force field, the TraPPE force field^{S6}, and the experimental values of Geier et al.^{S9}.

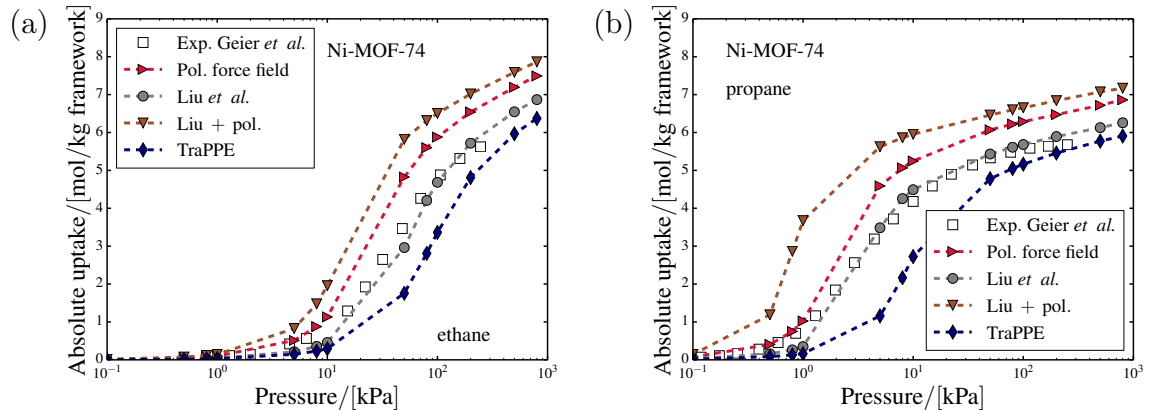


Figure S10: Adsorption isotherm for (a) ethane and (b) propane in Ni-MOF-74 at 318 K predicted with the force field of Liu *et al.*^{S1} with and without adding explicit polarization. Comparison with the polarizable force field, the TraPPE force field^{S6}, and the experimental values of Geier *et al.*^{S9}.

Force field parameters, heats of adsorption, and adsorption isotherms for Co-MOF-74 with QEq charges

Table S13: Force field parameters for Co-MOF-74 with charges calculated with the charge equilibration (QEq) method^{S10,S11}. The framework is considered to be rigid.

#	Atom type	ε / k_B [K]	σ [\text{\AA}]	Partial charge [e]
1	Co	7.045	2.56	1.162
2	O1	47.86	3.473	-0.473
3	O2	47.86	3.473	-0.531
4	O3	47.86	3.473	-0.585
5	C1	48.19	3.033	0.423
6	C2	48.19	3.033	-0.180
7	C3	48.19	3.033	0.209
8	C4	48.19	3.033	-0.108
9	H	7.65	2.846	0.083

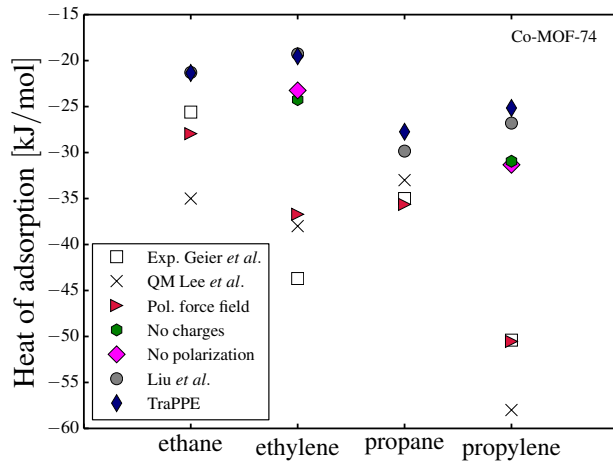


Figure S11: Heats of adsorption for Co-MOF-74 at infinite dilution calculated at 318 K with various force fields. The computational results are compared to DFT binding energies from Lee *et al.*^{S3} and heats of adsorption predicted via the Clausius-Clapeyron equation by Geier *et al.*^{S9}.

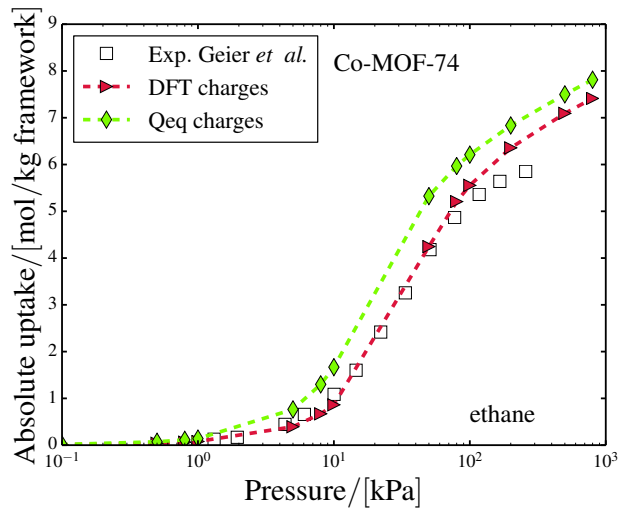


Figure S12: Adsorption isotherm for ethane at 318 K predicted with the developed polarizable force field and charges determined via (triangles) DFT calculations, and (diamonds) the QEq method.

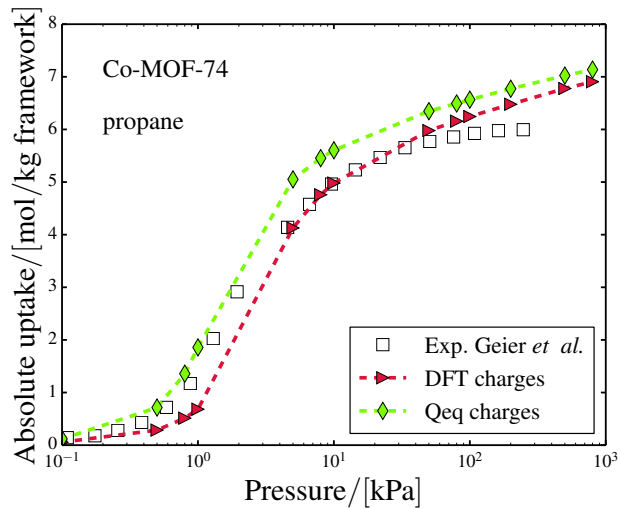


Figure S13: Adsorption isotherm for propane at 318 K predicted with the developed polarizable force field and charges determined via (triangles) DFT calculations, and (diamonds) the QEq method.

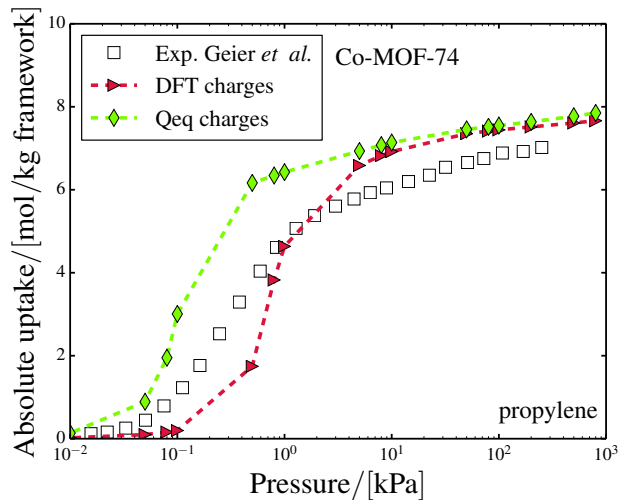


Figure S14: Adsorption isotherm for propylene at 318 K predicted with the developed polarizable force field and charges determined via (triangles) DFT calculations, and (diamonds) the QEq method.

Energy surfaces of Co-MOF-74 for the maximum energy plane in the z-direction

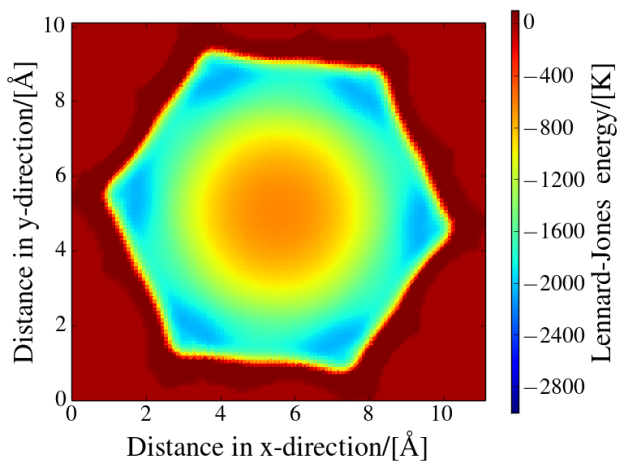


Figure S15: Lennard-Jones energies evaluated on a grid with 0.1 \AA spacing on the maximum energy plane in z-direction for ethylene in Co-MOF-74. Grid points for which the total energy (in units of k_B) is larger than 100 K are represented in dark red.

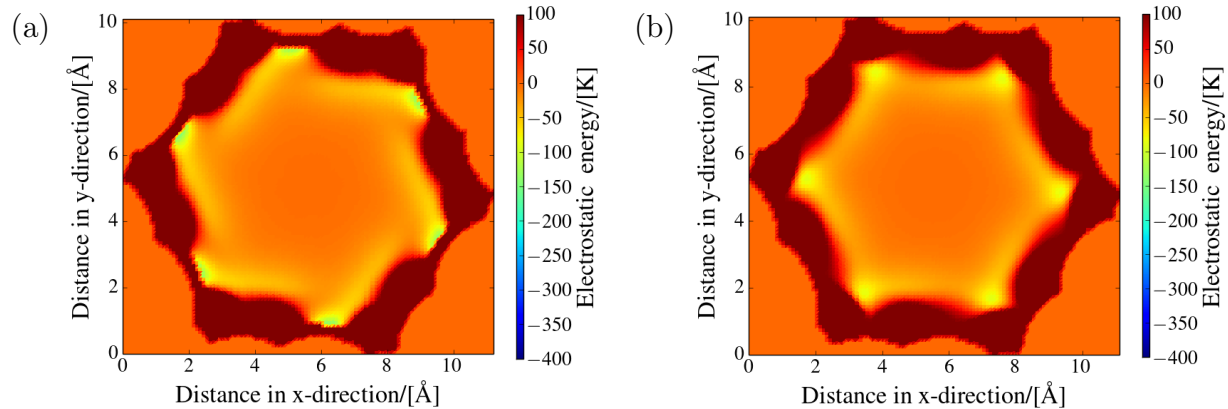


Figure S16: Comparison between the electrostatic energies for ethylene in Co-MOF-74 on a grid with (a) DFT charges and (b) charges calculated with the QEeq method for the plane of maximum energy. Grid points for which the total energy (in units of k_B) is larger than 100 K are represented in dark red.

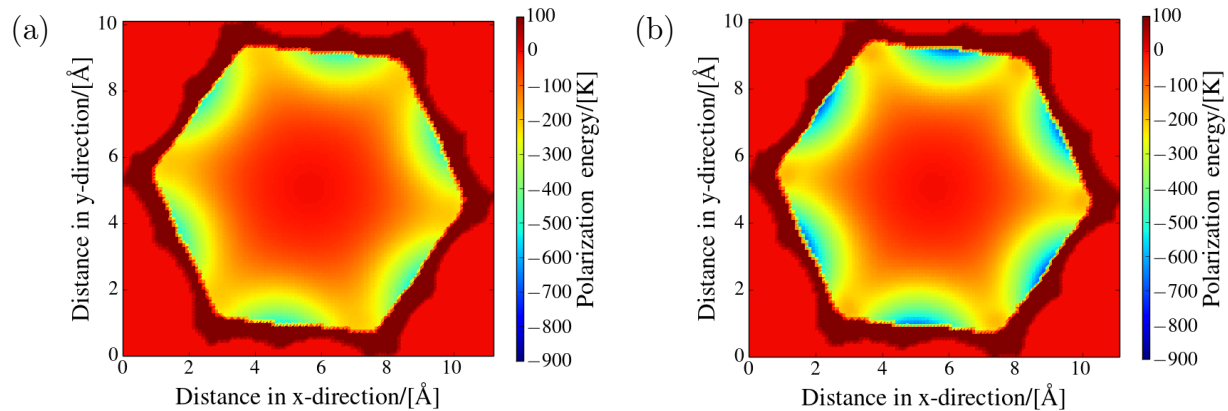


Figure S17: Comparison between the polarization energies for ethylene in Co-MOF-74 on a grid with (a) DFT charges and (b) charges calculated with the QEeq method for the plane of maximum energy. Grid points for which the total energy (in units of k_B) is larger than 100 K are represented in dark red.

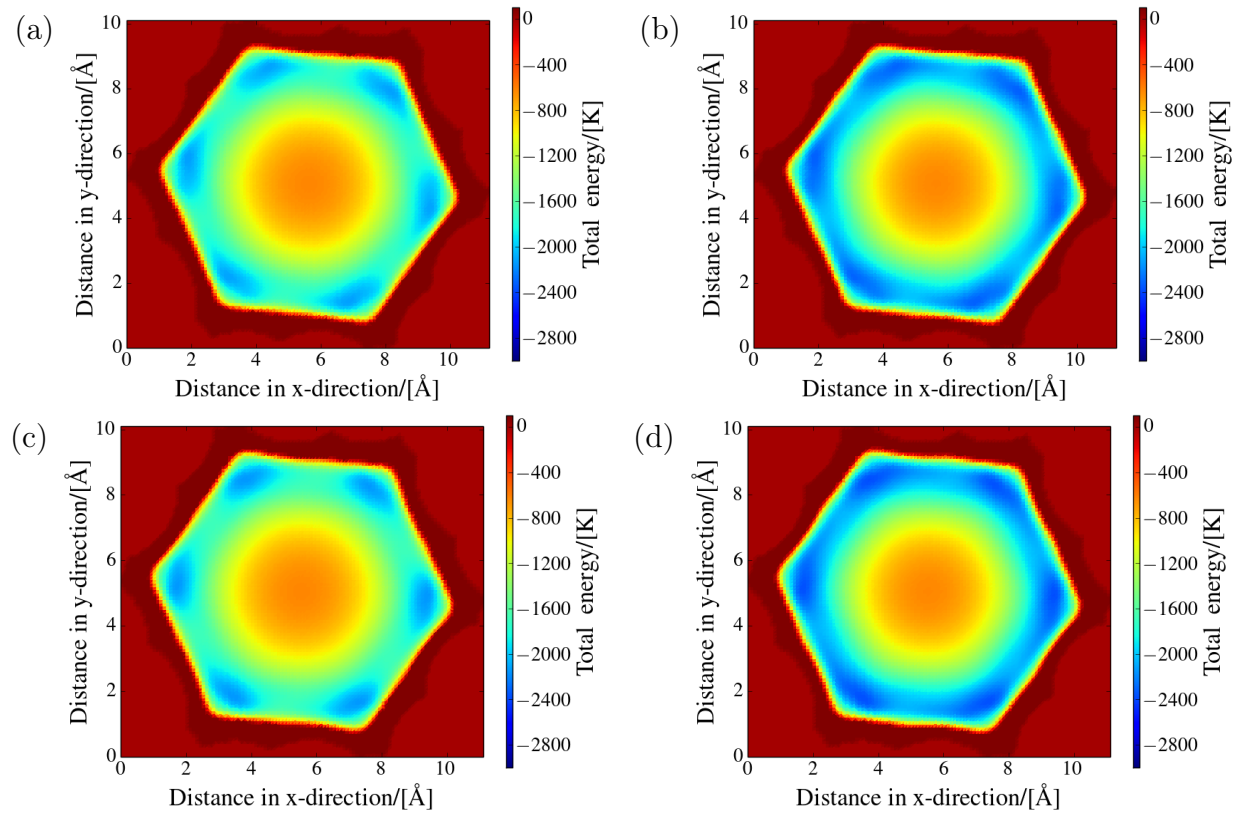


Figure S18: Comparison between the total energies for ethylene in Co-MOF-74 on a grid (left) without and (right) with explicit consideration of polarization energy. Energies calculated with (a) and (b) DFT charges and (c) and (d) charges calculated with the QEeq method for the plane of maximum energy. Grid points for which the total energy (in units of k_B) is larger than 100 K are represented in dark red.

References

- (S1) Liu B.; Smit B.; Rey F.; Valencia S.; Calero S. A New United Atom Force Field for Adsorption of Alkenes in Zeolites. *J. Phys. Chem. C* **2008**, *112*, 2492–2498.
- (S2) Lin, L.-C.; Lee, K.; Gagliardi, L.; Neaton, J. B.; Smit, B. Force-Field Development from Electronic Structure Calculations with Periodic Boundary Conditions: Applications to Gaseous Adsorption and Transport in Metal-Organic Frameworks. *J. Chem. Theory Comput.* **2014**, *10*, 1477–1488.
- (S3) Lee, K.; Howe, J. D.; Lin, L.-C.; Smit, B.; Neaton, J. B. Small-Molecule Adsorption in Open-Site Metal-Organic Frameworks: A Systematic Density Functional Theory Study for Rational Design. *Chem. Mater.* **2015**, *27*, 668–678.
- (S4) Mercado, R.; Vlaisavljevich, B.; Lin, L.-C.; Lee, K.; Lee, Y.; Mason, J. A.; Xiao, D. J.; Gonzalez, M. I.; Kapelewski, M. T.; Neaton, J. B., et al. Force Field Development from Periodic Density Functional Theory Calculations for Gas Separation Applications Using Metal-Organic Frameworks. *J. Phys. Chem. C* **2016**, *120*, 12590–12604.
- (S5) Stout, J. M.; Dykstra, C. E. Static Dipole Polarizabilities of Organic Molecules. Ab Initio Calculations and a Predictive Model. *J. Am. Chem. Soc.* **1995**, *117*, 5127–5132.
- (S6) Wick, C. D.; Martin, M. G.; Siepmann, J. I. Transferable Potentials for Phase Equilibria. 4. United-Atom Description of Linear and Branched Alkenes and Alkylbenzenes. *J. Phys. Chem. B* **2000**, *104*, 8008–8016.
- (S7) Lahoz-Martín, F. D.; Calero, S.; Gutiérrez-Sevillano, J. J.; Martín-Calvo, A. Adsorptive Separation of Ethane and Ethylene using IsoReticular Metal-Organic Frameworks. *Micropor. Mesopor. Mat.* **2017**, *248*, 40 – 45.
- (S8) Gutiérrez-Sevillano, J. J.; Dubbeldam, D.; Rey, F.; Valencia, S.; Palomino, M.; Martín-Calvo, A.; Calero, S. Analysis of the ITQ-12 Zeolite Performance in Propane-

Propylene Separations Using a Combination of Experiments and Molecular Simulations. *J.Phys. Chem. C* **2010**, *114*, 14907–14914.

- (S9) Geier, S. J.; Mason, J. A.; Bloch, E. D.; Queen, W. L.; Hudson, M. R.; Brown, C. M.; Long, J. R. Selective Adsorption of Ethylene over Ethane and Propylene over Propane in the Metal-Organic Frameworks $M_2(\text{dobdc})$ ($M = \text{Mg, Mn, Fe, Co, Ni, Zn}$). *Chem. Sci.* **2013**, *4*, 2054–2061.
- (S10) Rappe, A. K.; Goddard, W. A. Charge Equilibration for Molecular-Dynamics Simulations. *J. Phys. Chem.* **1991**, *95*, 3358–3363.
- (S11) Haldoupis, E.; Nair, S.; Sholl, D. S. Finding MOFs for Highly Selective CO_2/N_2 Adsorption Using Materials Screening Based on Efficient Assignment of Atomic Point Charges. *J. Am. Chem. Soc.* **2012**, *134*, 4313–4323.